

## RESEARCH LETTER

10.1002/2015GL066853

## Key Points:

- Highest nitrous oxide production occurs at the oxic-anoxic interface
- Denitrification controls the distribution of nitrous oxide in the oxygen minimum zone
- Nitrous oxide yield increases significantly with decreasing oxygen concentrations

## Supporting Information:

- Supporting Information S1

## Correspondence to:

Q. Ji,  
qji@princeton.edu

## Citation:

Ji, Q., A. R. Babbin, A. Jayakumar, S. Oleynik, and B. B. Ward (2015), Nitrous oxide production by nitrification and denitrification in the Eastern Tropical South Pacific oxygen minimum zone, *Geophys. Res. Lett.*, *42*, 10,755–10,764, doi:10.1002/2015GL066853.

Received 2 NOV 2015

Accepted 2 DEC 2015

Accepted article online 10 DEC 2015

Published online 19 DEC 2015

## Nitrous oxide production by nitrification and denitrification in the Eastern Tropical South Pacific oxygen minimum zone

Qixing Ji<sup>1</sup>, Andrew R. Babbin<sup>2</sup>, Amal Jayakumar<sup>1</sup>, Sergey Oleynik<sup>1</sup>, and Bess B. Ward<sup>1</sup>

<sup>1</sup>Department of Geosciences, Guyot Hall, Princeton University, Princeton, NJ, USA, <sup>2</sup>Department of Civil & Environmental Engineering, Massachusetts Institute of Technology, Cambridge, Massachusetts, USA

**Abstract** The Eastern Tropical South Pacific oxygen minimum zone (ETSP-OMZ) is a site of intense nitrous oxide (N<sub>2</sub>O) flux to the atmosphere. This flux results from production of N<sub>2</sub>O by nitrification and denitrification, but the contribution of the two processes is unknown. The rates of these pathways and their distributions were measured directly using <sup>15</sup>N tracers. The highest N<sub>2</sub>O production rates occurred at the depth of peak N<sub>2</sub>O concentrations at the oxic-anoxic interface above the oxygen deficient zone (ODZ) because slightly oxygenated waters allowed (1) N<sub>2</sub>O production from both nitrification and denitrification and (2) higher nitrous oxide production yields from nitrification. Within the ODZ proper (i.e., anoxia), the only source of N<sub>2</sub>O was denitrification (i.e., nitrite and nitrate reduction), the rates of which were reflected in the abundance of *nirS* genes (encoding nitrite reductase). Overall, denitrification was the dominant pathway contributing the N<sub>2</sub>O production in the ETSP-OMZ.

### 1. Introduction

Nitrous oxide (N<sub>2</sub>O) is important to Earth's climate because it is a strong radiation absorber and an ozone depletion agent. The recent Intergovernmental Panel on Climate Change (IPCC) report estimates that N<sub>2</sub>O emissions to the atmosphere from the open ocean are ~3.8 Tg N yr<sup>-1</sup>, ~35% of total natural emissions [Ciais *et al.*, 2013]. The highest oceanic N<sub>2</sub>O effluxes occur in regions called oxygen minimum zones (OMZs) in the Eastern Tropical Pacific [Cohen and Gordon, 1978; Arevalo-Martinez *et al.*, 2015] and the Arabian Sea [Law and Owens, 1990; Naqvi and Noronha, 1991]. These OMZs are characterized by steep dissolved oxygen (O<sub>2</sub>) gradients (oxycines) sandwiching a layer of significant nitrite accumulation (>1 μM), which indicates anoxia ([O<sub>2</sub>] <10 nM) [Revsbech *et al.*, 2009; Thamdrup *et al.*, 2012]. This layer of essentially zero [O<sub>2</sub>] is referred to as the oxygen deficient zone (ODZ). At the oxic-anoxic interfaces above and below the ODZ, N<sub>2</sub>O concentrations exceed saturation by several fold, which has presumably persisted over decades [Babbin *et al.*, 2015].

Active N<sub>2</sub>O production is necessary for the persistence of this subsurface N<sub>2</sub>O supersaturation. The existing gradients of inorganic nitrogen substrates and oxygen in the OMZs can support two possible microbial pathways for N<sub>2</sub>O production, nitrification and denitrification.

**Nitrification.** In the presence of molecular oxygen, ammonium (NH<sub>4</sub><sup>+</sup>) is oxidized to nitrite (NO<sub>2</sub><sup>-</sup>) via hydroxylamine (NH<sub>2</sub>OH) by ammonia oxidizing bacteria (AOB), with N<sub>2</sub>O as a by-product [Anderson, 1964]. Ammonia oxidizing archaea (AOA) also produce N<sub>2</sub>O by pathways that are apparently similar but less well understood [Stieglmeier *et al.*, 2014]. This nitrification-derived N<sub>2</sub>O production pathway in marine environments has been substantiated by a positive correlation between apparent oxygen utilization and N<sub>2</sub>O concentration excess [Cohen and Gordon, 1978] and by active production of <sup>15</sup>N<sub>2</sub>O in <sup>15</sup>N tracer incubation experiments [Yoshida *et al.*, 1989]. Nitrification could be an especially significant source of N<sub>2</sub>O in the OMZs because the yield of N<sub>2</sub>O during nitrification, i.e., the ratio of N<sub>2</sub>O production to NO<sub>2</sub><sup>-</sup> production, increases dramatically with decreasing O<sub>2</sub> concentration as demonstrated for cultivated AOB by Goreau *et al.* [1980] and for AOA by Löscher *et al.* [2012]. These data suggest that for natural assemblages in the oxycline, the N<sub>2</sub>O yield should increase as a result of decreasing oxygen concentration [Codispoti and Christensen, 1985].

**Denitrification.** Under anoxic and suboxic conditions ([O<sub>2</sub>] < 10 μM), nitrate (NO<sub>3</sub><sup>-</sup>) and NO<sub>2</sub><sup>-</sup> can be reduced by denitrifying bacteria to N<sub>2</sub>O through stepwise canonical denitrification. Naqvi *et al.* [2000] documented N<sub>2</sub>O accumulation in incubation experiments and <sup>15</sup>N-N<sub>2</sub>O production was detected in <sup>15</sup>NO<sub>2</sub><sup>-</sup> and <sup>15</sup>NO<sub>3</sub><sup>-</sup>

tracer experiments in the Arabian Sea [Nicholls et al., 2007] and the Eastern Tropical South Pacific (ETSP) OMZ [Dalsgaard et al., 2012]. The series of enzymes mediating the process—nitrate reductase, nitrite reductase, nitric oxide reductase, and nitrous oxide reductase—are progressively less oxygen tolerant [Körner and Zumft, 1989]. Thus, under a certain oxygen concentration, reduction of  $\text{NO}_3^-$  and  $\text{NO}_2^-$  could halt at  $\text{N}_2\text{O}$ , because the reduction of  $\text{N}_2\text{O}$  to  $\text{N}_2$  is inhibited by oxygen. This decoupling is suggested to contribute to the accumulation of  $\text{N}_2\text{O}$  by  $\text{NO}_3^-$  and  $\text{NO}_2^-$  reduction within the upper layer of the ODZ and the overlying oxycline [Babbin et al., 2015]. A partial denitrification pathway is also carried out by AOB that possess the nitrite and nitric oxide reductase enzymes. AOB reduce  $\text{NO}_2^-$  to  $\text{N}_2\text{O}$  under low-oxygen conditions, a process termed “nitrifier denitrification” [Poth and Focht, 1985; Frame and Casciotti, 2010]. Nitrifier denitrification was observed in the oxygenated North Pacific subtropical gyre tracing  $^{15}\text{N}$  transfer from  $\text{NO}_2^-$  to  $\text{N}_2\text{O}$  [Wilson et al., 2014]. Characteristically, nitrifier denitrification only reduces  $\text{NO}_2^-$ , whereas both  $\text{NO}_3^-$  and  $\text{NO}_2^-$  can be utilized by denitrifiers.

In the ETSP-OMZ,  $\text{NH}_4^+$ ,  $\text{NO}_2^-$ , and  $\text{NO}_3^-$  are present in the steep oxygen gradients overlying the ODZ, supporting both nitrification and denitrification. Oxygen level is probably an important factor regulating the relative contributions of nitrification and denitrification in  $\text{N}_2\text{O}$  production in OMZs [Codispoti and Christensen, 1985].  $\text{N}_2\text{O}$  production rates and pathways have been modeled to estimate global fluxes using water column concentration data (e.g. Freing et al. [2012]). However, field studies investigating the relative contributions of different  $\text{N}_2\text{O}$  production pathways and the regulating environmental factors would be useful for (1) improving  $\text{N}_2\text{O}$  models in representing biogeochemical  $\text{N}_2\text{O}$  cycling processes in marine environments, (2) reducing the uncertainty of the magnitude of marine  $\text{N}_2\text{O}$  production rates, and (3) providing insights into future  $\text{N}_2\text{O}$  production in the ocean in response to changing climate. The present study was designed to capture the  $\text{N}_2\text{O}$  production dynamics in OMZs. Incubation experiments with  $^{15}\text{N}$  tracers ( $^{15}\text{NH}_4^+$ ,  $^{15}\text{NO}_2^-$ , and  $^{15}\text{NO}_3^-$ ) were performed to directly measure  $\text{N}_2\text{O}$  production. Nitrification-derived  $\text{N}_2\text{O}$  production is operationally defined as  $^{15}\text{N}_2\text{O}$  production from  $^{15}\text{NH}_4^+$ -spiked incubations. This definition focuses on the oxidative  $\text{N}_2\text{O}$  production pathways and implies the requirement for oxygen. This nitrification source potentially includes two known mechanisms by which  $\text{N}_2\text{O}$  is produced by ammonia oxidizers:  $\text{N}_2\text{O}$  produced from the hydroxylamine intermediate and  $\text{N}_2\text{O}$  produced by reduction of the  $\text{NO}_2^-$  derived from  $^{15}\text{NH}_4^+$  oxidation.  $^{15}\text{N}_2\text{O}$  produced in  $^{15}\text{NO}_2^-$ - and  $^{15}\text{NO}_3^-$ -spiked incubations defines the denitrification counterpart, as the reductive  $\text{N}_2\text{O}$  production pathways mediated by both nitrifiers and denitrifiers. In addition, the abundance of *nirS* genes, encoding nitrite reductase, was analyzed in relation to measured rates of  $\text{NO}_3^-$  and  $\text{NO}_2^-$  reduction to  $\text{N}_2\text{O}$ . These data could (1) determine the relative significance of nitrification compared with denitrification in  $\text{N}_2\text{O}$  production in the OMZs and (2) improve the accuracy of global marine  $\text{N}_2\text{O}$  production models by better characterizing  $\text{N}_2\text{O}$  yield during nitrification by natural assemblages rather than pure cultures in oxygenated waters where nitrification is a major pathway [Suntharalingam and Sarmiento, 2000; Nevison et al., 2003; Bianchi et al., 2012; Zamora and Oschlies, 2014].

## 2. Experiments and Methods

### 2.1. Study Site

Shipboard sampling and incubation were carried out on the R/V *Nathaniel B. Palmer* during June–July 2013 (NBP 1305). Samples were collected from the upper oxycline at seven transect stations and from complete depth profiles at two process stations parallel to the coast between 21.5°S and 13.0°S. Process station BB1 and BB2 represent offshore and coastal environments, respectively (Figure S1 in the supporting information).

### 2.2. Water Column Profiles

Water was collected in 12 L Niskin bottles mounted on a standard conductivity-temperature-depth (CTD) rosette system. An oxygen sensor (Seabird SBE43, Bellevue, WA) calibrated by Winkler titration (detection limit 2.1  $\mu\text{M}$ ) and a real-time STOX sensor (detection limit 10 nM; Revsbech et al. [2009]) were deployed on the CTD. Nutrients ( $\text{NO}_2^-$  and  $\text{NO}_3^-$ ) were measured onboard using standard colorimetric protocols established by United Nations Educational, Scientific and Cultural Organization [1994], with detection limits of 0.02  $\mu\text{M}$ . The protocol for determining  $\text{NH}_4^+$  concentration was modified from Mantoura and Woodward [1983], with a detection limit of 0.01  $\mu\text{M}$ . Discrete samples for  $\text{N}_2\text{O}$  concentrations were collected from Niskin bottles into acid-washed, 60 mL glass serum bottles (Wheaton, Millville, NJ) by flushing with three

volumes and sealed with a 20 mm three-prong butyl stopper (Wheaton, Millville, NJ) and an aluminum crimp seal (National Scientific, Rockwood, TN) without headspace. Within 20 min of collection, 5 mL of headspace was created with ultrahigh purity (UHP) helium (Airgas, Radnor, PA). Samples were preserved by adding 0.1 mL of saturated mercuric chloride ( $\text{HgCl}_2$ , Thermo Fisher Scientific, Waltham, MA) and stored in the dark until analysis.

### 2.3. Tracer Incubations for $\text{N}_2\text{O}$ Production

Comprehensive  $\text{N}_2\text{O}$  production rate measurements were completed at the two process stations (Station BB1, 14.00°S, 81.20°W, bottom depth 4890 m; Station BB2, 20.50°S, 70.70°W, bottom depth 1790 m) representing offshore and coastal environments, respectively. The sampling depths were chosen to target specific water column features such as sharp  $[\text{O}_2]$  gradients and local  $[\text{NO}_2^-]$  maxima (Figures 1a and 1b). Seawater was sampled into 60 mL glass serum bottles using the same procedure described above for  $\text{N}_2\text{O}$  concentration samples (section 2.2). Headspace (5 mL) was created by replacing the volume with UHP helium. Three suites of solutions ( $^{15}\text{NH}_4^+$  plus  $^{14}\text{NO}_2^-$ ,  $^{15}\text{NO}_2^-$  plus  $^{14}\text{NH}_4^+$ ,  $^{15}\text{NO}_3^-$  plus  $^{14}\text{NH}_4^+$ , and  $^{14}\text{NO}_2^-$ , 0.1 mL total volume) consisting of  $^{15}\text{N}$  tracer (99% purity, Cambridge Isotope, Tewksbury, MA) and  $^{14}\text{N}$  carrier (ACS grade, Thermo Fisher Scientific, Waltham, MA) were added to separate bottles in triplicate to enrich  $^{15}\text{NH}_4^+$ ,  $^{15}\text{NO}_2^-$ , and  $^{15}\text{NO}_3^-$  by 0.5, 1.0, and 1.0  $\mu\text{M}$  (final concentration), respectively. These combinations of  $^{15}\text{N}$  and  $^{14}\text{N}$  solutions were designed to increase nitrogen substrate concentrations to similar levels to avoid differential stimulation of different processes. Nitrogen-15 enrichments of the initial substrate pools were usually >95%, 15–95%, and <10% for  $\text{NH}_4^+$ ,  $\text{NO}_2^-$ , and  $\text{NO}_3^-$ , respectively. Tracer solutions were made from deionized water, and were degassed prior to incubation. Incubations lasted 24–36 h in a temperature-controlled environment close to ( $\pm 3^\circ\text{C}$ ) in situ temperatures and were terminated by adding 0.1 mL of saturated  $\text{HgCl}_2$  solution.

The effect of oxygen concentrations on  $\text{N}_2\text{O}$  production during nitrification and denitrification was further investigated at the upper boundary of the ODZ (80 m) at the coastal process station BB2 ( $[\text{O}_2] < 10 \text{ nM}$ ). Samples were acquired using a pump profiling system (PPS) equipped with a CTD package, an oxygen sensor (SBE-25, Seabird Electronics, Bellevue, WA), and a real-time STOX unit as previously described by *Canfield et al.* [2010]. The PPS minimized oxygen contamination during sampling and allowed better representation of in situ anoxic conditions during incubation experiments. After the serum bottles were filled directly from the pump outlet, sealed and 5 mL helium headspace created, volumes of 0, 0.5, and 2 mL of  $\text{O}_2$  saturated site water ( $\sim 225 \mu\text{M}$ ) were injected into the sealed incubation bottles through the rubber septum to attain <0.01, 2.25, and 9  $\mu\text{M}$   $[\text{O}_2]$ , concentrations representing those in the oxycline. The same suite of degassed tracers as above was utilized, and incubations lasted 24 h at in situ temperature ( $12^\circ\text{C}$ ) before termination with  $\text{HgCl}_2$ .

Preserved samples were stored in the dark for less than 6 months before analysis.  $\text{N}_2\text{O}$  was extracted by purging with helium for 40 min at a rate of  $37 \text{ mL min}^{-1}$  and subsequently trapped by liquid nitrogen and isolated from interference by gas chromatography. Pulses of sample  $\text{N}_2\text{O}$  were injected into an isotope ratio mass spectrometer (Delta V<sup>Plus</sup>; Thermo Scientific, Waltham, MA) for mass and isotope ratio ( $m/z = 44, 45, 46$ ) measurements.  $\text{N}_2\text{O}$  concentrations were calculated using the measured amount of  $\text{N}_2\text{O}$  divided by the volume of seawater ( $54 \pm 0.4 \text{ mL}$ ). A standard curve of  $\text{N}_2\text{O}$  concentrations was generated from standard injections of 1, 2, 5, 10, 15, and 20 nmol  $\text{N}_2\text{O-N}$  into serum bottles containing 54 mL of He-flushed seawater.  $\text{N}_2\text{O}$  production from  $^{15}\text{N}$  labeled substrate was quantified as the increase in  $^{45}\text{N}_2\text{O}$  and  $^{46}\text{N}_2\text{O}$  at the end of the incubation with respect to natural abundance.  $\text{N}_2\text{O}$  production rates ( $R_{\text{N}_2\text{O}}$ , in  $\text{nM-N d}^{-1}$ ) were calculated according to the following:

$$R_{\text{N}_2\text{O}} = \frac{[^{45}\text{N}_2\text{O}]_{t_1} - [^{45}\text{N}_2\text{O}]_{t_0}}{F \times \Delta t} + 2 \times \frac{[^{46}\text{N}_2\text{O}]_{t_1} - [^{46}\text{N}_2\text{O}]_{t_0}}{F \times \Delta t} \quad (1)$$

where  $[^{45,46}\text{N}_2\text{O}]_{t_1,t_0}$  represent the rates of masses 45 and 46  $\text{N}_2\text{O}$  concentration at the end ( $t_1$ ) and start ( $t_0$ ) of incubation.  $F$  represents the fraction of  $^{15}\text{N}$  in the initial substrate pool ( $\text{NH}_4^+$ ,  $\text{NO}_2^-$ , or  $\text{NO}_3^-$ ), and  $\Delta t$  is incubation time. The mass spectrometer detection limit of the  $\text{N}_2\text{O}$  production is  $0.005 \text{ nM d}^{-1}$ .

### 2.4. Measurement of $\text{NO}_2^-$ Production

$\text{NO}_2^-$  production rates were measured in samples enriched with  $^{15}\text{NH}_4^+$  or  $^{15}\text{NO}_3^-$ , using the azide reduction method [*McIlvin and Altabet*, 2005]. Seawater (5 mL) was transferred using 5 mL gas-tight glass syringe

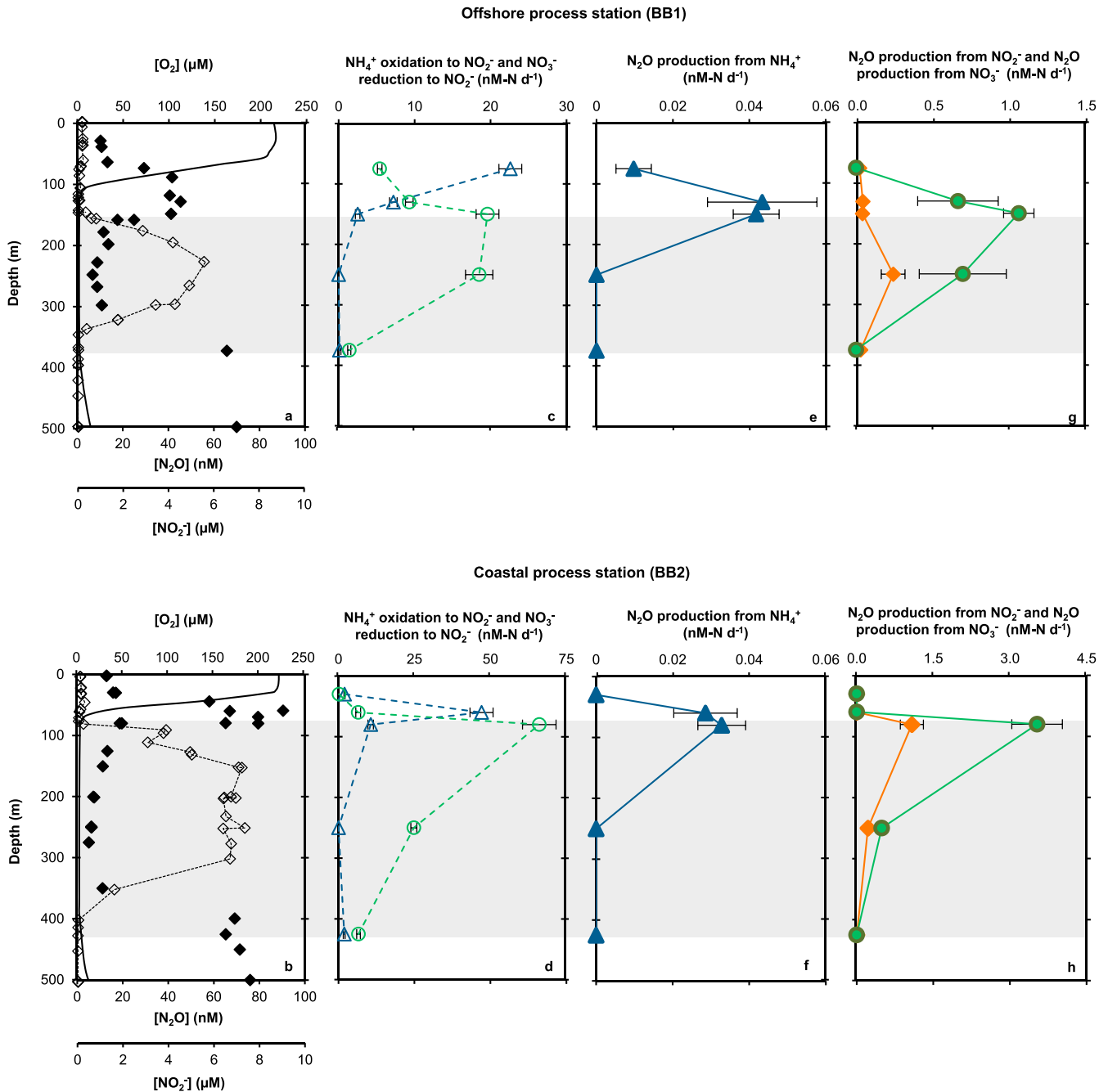


**Figure 1.** (a and b) Vertical concentration profiles of dissolved oxygen (solid line), N<sub>2</sub>O (filled diamond), and NO<sub>2</sub><sup>-</sup> (empty diamond with dashed line). (c and d) Rates of NH<sub>4</sub><sup>+</sup> oxidation to NO<sub>2</sub><sup>-</sup> (triangles) and NO<sub>3</sub><sup>-</sup> reduction to NO<sub>2</sub><sup>-</sup> (circles). (e and f) Rates of N<sub>2</sub>O production from NH<sub>4</sub><sup>+</sup> oxidation. (g and h) Rates of N<sub>2</sub>O production from NO<sub>2</sub><sup>-</sup> reduction (diamonds) and NO<sub>3</sub><sup>-</sup> reduction (circles). Data from (Figures 1a, 1c, 1e, and 1g) offshore process station BB1 and (Figures 1b, 1d, 1f, and 1h) coastal process station BB2. Shaded areas represent oxygen deficient zone ([O<sub>2</sub>] < 10 nM). Error bars represent standard deviation of rates determined from linear fit of time course measurements.

(Hamilton Co., Reno, NV) from serum bottles to He-flushed 20 mL vials (Grace Co., Columbia, MD). The acetic acid-treated sodium azide solution quantitatively converted NO<sub>2</sub><sup>-</sup> to N<sub>2</sub>O. The resulting N<sub>2</sub>O was measured using a mass spectrometer as previously described. Rates were calculated as

$$R_{NO_2^-} = \frac{[^{15}NO_2^-]_{t1} - [^{15}NO_2^-]_{t0}}{F \times \Delta t} \quad (2)$$

where  $[^{15}\text{NO}_2^-]_{t1,t0}$  represent  $^{15}\text{NO}_2^-$  concentration at the end and start of the incubation, respectively;  $F$  represents the fraction of  $^{15}\text{N}$  in the initial substrate pool ( $\text{NH}_4^+$  or  $\text{NO}_3^-$ ), and  $\Delta t$  is incubation time. The detection limit for the  $\text{NO}_2^-$  production rates is  $0.01 \text{ nM d}^{-1}$ .

$\text{N}_2\text{O}$  production and  $\text{NO}_2^-$  production were measured in seawater incubations with  $^{15}\text{NH}_4^+$  as described above. The  $\text{N}_2\text{O}$  yield was defined as the ratio of  $\text{N}_2\text{O}$  to  $\text{NO}_2^-$  production during  $\text{NH}_4^+$  oxidation.

### 2.5. Water Column qPCR *nirS* Analysis

Methods of DNA extraction and qPCR for the *nirS* gene using SYBR Green have been described previously by Jayakumar *et al.* [2009, 2013]. Standardization and verification of specificity for quantitative PCR assays were performed as described in Jayakumar *et al.* [2013]. The efficiency of the qPCR reactions was calculated using the slopes of the standard curves; the efficiency ranged between 85 and 106%. The amplified products were visualized after electrophoresis in ethidium bromide stained 1.0% agarose gels and were further confirmed by cloning and sequencing the PCR product. Standards for PCR quantification of each fragment were prepared by amplifying a constructed plasmid containing the respective gene fragment, followed by quantification and serial dilution. Assays were carried out in a single assay plate [Smith *et al.*, 2006] for each gene with DNA samples (20–25 ng), from all depths in triplicates and also included no template controls, no primer control, four or more dilution of standards. DNA was quantified using PicoGreen fluorescence (Molecular Probes, Eugene, and OR) calibrated with several dilutions of phage lambda standards and qPCR was performed using a Stratagene MX3000P (Agilent Technologies, La Jolla, CA). Automatic analysis settings were used to determine the threshold cycle values. To account for DNA loss that occurs upon repeated freeze-thaw cycles, plasmid DNA and environmental DNA was quantified prior to every assay.

## 3. Results and Discussion

### 3.1. $\text{N}_2\text{O}$ Production and Accumulation at the Oxidic-Anoxic Interface

Both the offshore and coastal sampling stations were characterized by water column  $\text{N}_2\text{O}$  supersaturation at the surface (~150% saturation) and in the upper oxycline (>400% saturation), confirming that the region is important for oceanic  $\text{N}_2\text{O}$  production (Figures 1a and 1b). The peak  $\text{N}_2\text{O}$  concentrations at the oxidic-anoxic interface suggest that this depth interval has unique conditions suitable for  $\text{N}_2\text{O}$  production and accumulation.

#### 3.1.1. Ammonium Oxidation

The highest rates of  $\text{NH}_4^+$  oxidation to  $\text{NO}_2^-$  ( $22\text{--}47 \text{ nM-N d}^{-1}$ ) occurred at the upper oxycline (Figures 1c and 1d) and thus contributed to the small upper (primary)  $\text{NO}_2^-$  maximum with  $[\text{NO}_2^-]$  of  $0.2\text{--}0.3 \mu\text{M}$  (~60 m, Figures 1a and 1b). However, the highest rates of  $\text{NH}_4^+$  oxidation to  $\text{NO}_2^-$  did not always coincide with the highest rates of  $\text{NH}_4^+$  oxidation to  $\text{N}_2\text{O}$ , which were detected at the peak  $[\text{N}_2\text{O}]$  near the oxidic-anoxic interface, with rates between  $0.02$  and  $0.04 \text{ nM d}^{-1}$  (Figures 1e and 1f). At the secondary nitrite maximum (SNM) where in situ  $[\text{O}_2] < 10 \text{ nM}$ ,  $\text{NH}_4^+$  oxidation was below detection limit. Rates were low in the surface euphotic layer (30 m at station BB2) where  $[\text{NH}_4^+]$  was generally high ( $>0.5 \mu\text{M}$ ) (Figure S2).

These data from the ETSP-OMZ revealed that nitrification-derived  $\text{N}_2\text{O}$  production peaked at the oxidic-anoxic interface. Fundamentally, the  $\text{N}_2\text{O}$  production rate depends on the  $\text{NO}_2^-$  production rate and is modulated by the constraints of the light,  $\text{NH}_4^+$  availability, and  $\text{O}_2$  distributions. The depth of the  $\text{NH}_4^+$  oxidation rate maximum is likely the result of release from light inhibition, at a depth with adequate  $\text{NH}_4^+$  supply and  $[\text{O}_2]$ , i.e., between the base of the euphotic zone and the top of the ODZ [Codispoti and Christensen, 1985; Lipschultz *et al.*, 1990; Molina and Farías, 2009]. The oxidation of  $\text{NH}_4^+$  is inhibited by one or more factors in other depth ranges: (1) In the surface euphotic zone, nitrifiers are inhibited by light and are not competitive in  $\text{NH}_4^+$  uptake when phytoplankton are present [Ward, 2005]. (2) Within the ODZ, lack of oxygen inhibits growth of nitrifiers. (3) Below the ODZ, low nitrification rates probably result from low supply of  $\text{NH}_4^+$  [Ward and Zafriou, 1988]. In addition,  $\text{NH}_4^+$  oxidation was also detected at the top of the ODZ where in situ  $[\text{O}_2] < 10 \text{ nM}$  (Figures 1a and 1b). This could be due to contamination by atmospheric oxygen with  $\sim 0.5 \mu\text{M} [\text{O}_2]$  [De Brabandere *et al.*, 2012] during shipboard CTD sampling, but it also suggests that nitrifiers were primed to oxidize  $\text{NH}_4^+$  at low oxygen concentrations [Martens-Habbena *et al.*, 2009].

### 3.1.2. Nitrite and Nitrate Reduction

The first step of denitrification,  $\text{NO}_3^-$  reduction to  $\text{NO}_2^-$ , was detected at the SNM and in the upper oxycline, with the highest rates (up to  $66 \text{ nM-N d}^{-1}$ ) at the top of the ODZ. High rates of  $\text{NO}_3^-$  reduction to  $\text{NO}_2^-$  within the ODZ contributed to the accumulation of  $\text{NO}_2^-$  (up to  $7 \mu\text{M}$ ) and the corresponding local  $\text{NO}_3^-$  minimum (Figure S2).

The production of  $\text{N}_2\text{O}$  from denitrification ( $\text{N}_2\text{O}$  production from both  $\text{NO}_2^-$  and  $\text{NO}_3^-$  reduction) was detected within the ODZ and at the base of the oxycline at the offshore process station. At these depth intervals, over 90% of  $\text{N}_2\text{O}$  production was from denitrification, with rates of  $\text{NO}_2^-$  reduction plus  $\text{NO}_3^-$  reduction to  $\text{N}_2\text{O}$  exceeding  $0.7 \text{ nM-N d}^{-1}$ . At the oxycline below the ODZ, despite relatively high  $\text{N}_2\text{O}$  concentrations ( $\sim 70 \text{ nM}$ ),  $\text{N}_2\text{O}$  production was only detected from  $\text{NO}_2^-$  reduction, at rates of  $\sim 0.02 \text{ nM d}^{-1}$ . The experimental design cannot distinguish nitrifier denitrification from denitrifier denitrification, but the fact that  $\text{N}_2\text{O}$  production from  $\text{NO}_3^-$  usually exceeded  $\text{N}_2\text{O}$  production from  $\text{NO}_2^-$  (Figures 1g and 1h) leaves no doubt that denitrifier denitrification was the dominant process.

If both  $\text{NO}_3^-$  and  $\text{NO}_2^-$  reduction to  $\text{N}_2\text{O}$  represent denitrification, it is not clear why  $\text{NO}_3^-$  reduction rates should exceed  $\text{NO}_2^-$  reduction rates. Organic matter—the electron donor—is considered the limiting substrate for water column denitrification [Ward *et al.*, 2008; Babbín *et al.*, 2014]. The free energy gain, in terms of organic matter oxidation, under in situ conditions for  $\text{NO}_3^-$  reduction to  $\text{N}_2\text{O}$  is less thermodynamically favorable than that of  $\text{NO}_2^-$  reduction (Text S1), suggesting that  $\text{NO}_2^-$  reduction should be preferred when both  $\text{NO}_2^-$  and  $\text{NO}_3^-$  are available. However, higher rates of  $\text{N}_2\text{O}$  production from  $\text{NO}_3^-$  imply that carbon limitation may not be the main control on the reductive  $\text{N}_2\text{O}$  production. As the intermediate during denitrification,  $\text{NO}_2^-$  is able to exchange in and out of the cells [Moir and Wood, 2001], but the dilution of tracer with ambient  $^{14}\text{NO}_2^-$  caused by this exchange should affect rates measured from  $^{15}\text{NO}_3^-$  incubations. It may be that the high concentration of  $\text{NO}_3^-$  in these regions favors  $\text{NO}_3^-$  reduction by denitrifiers.

Denitrification, indicated by  $\text{NO}_2^-$  and  $\text{NO}_3^-$  reduction to  $\text{N}_2\text{O}$  was apparently not affected by  $[\text{O}_2] < 10 \mu\text{M}$ . Under manipulated  $[\text{O}_2]$  between  $0.01$  and  $9 \mu\text{M}$ , rates of  $\text{NO}_3^-$  and  $\text{NO}_2^-$  reduction to  $\text{N}_2\text{O}$  were not statistically different (Figure S3). Thus,  $\text{NO}_3^-$  and  $\text{NO}_2^-$  reduction to  $\text{N}_2\text{O}$  could occur in the oxycline overlying the ODZ, and contribute significantly to  $\text{N}_2\text{O}$  production. This is in agreement with a modeling exercise that inferred  $\text{N}_2\text{O}$  production by oxycline denitrification in the Eastern tropical North Pacific OMZ [Babbín *et al.*, 2015].

Overall, the availability of  $\text{N}_2\text{O}$  production substrates,  $\text{NH}_4^+$ ,  $\text{NO}_2^-$ , and  $\text{NO}_3^-$ , coincided with suboxic conditions that allowed  $\text{NH}_4^+$  oxidation, and  $\text{NO}_2^-$  and  $\text{NO}_3^-$  reduction to cooccur. Using the water column  $\text{N}_2\text{O}$  production rates from denitrification of  $1 \pm 0.25 \text{ nM-N d}^{-1}$ , assuming the rates measured here represent average rates for OMZ regions, and that a  $10 \pm 4 \text{ m}$  thick layer above the ODZ is the interval where  $\text{N}_2\text{O}$  production from denitrification exceeds consumption [Babbín *et al.*, 2015], the  $\text{N}_2\text{O}$  production from denitrification within the OMZs is estimated to be  $10 \pm 5 \mu\text{mol of N m}^{-2} \text{ d}^{-1}$ . Assuming a layer of  $75 \pm 25 \text{ m}$  above the ODZ where nitrification is contributing to  $\text{N}_2\text{O}$  production at a production rate of  $0.03 \pm 0.01 \text{ nM-N d}^{-1}$ , the contribution of  $\text{N}_2\text{O}$  production from nitrification in the OMZs is  $2 \pm 1 \mu\text{mol of N m}^{-2} \text{ d}^{-1}$ . Thus, denitrification is the major pathway of  $\text{N}_2\text{O}$  production in the OMZ regions and potentially to global marine  $\text{N}_2\text{O}$  production.

### 3.2. The $\text{N}_2\text{O}$ Yield During Nitrification

The average  $\text{N}_2\text{O}$  yield was 0.04% when  $[\text{O}_2]$  was close to saturation. A nonlinear increase in  $\text{N}_2\text{O}$  yield was observed at lower  $[\text{O}_2]$ . The yield increased significantly at  $[\text{O}_2]$  below  $50 \mu\text{M}$ . Samples from the top of the ODZ had higher yield ( $> 1\%$ ); the maximum yield (1.6%) was a fortyfold increase compared to the typical yield for samples at  $[\text{O}_2] > 50 \mu\text{M}$ . Below the ODZ,  $\text{N}_2\text{O}$  production from nitrification was low to undetectable because  $\text{NO}_2^-$  production from nitrification was very slow; thus, the yield could not be determined. The direct measurement of  $\text{N}_2\text{O}$  yield (0.04–1.6%) in this study substantiated results from culture work showing a nonlinear increase in  $\text{N}_2\text{O}$  yield with decreasing in situ  $[\text{O}_2]$  [Goreau *et al.*, 1980]. The majority of the ocean volume is oxygenated and nitrification is likely to dominate the  $\text{N}_2\text{O}$  source in the ocean outside the OMZs, making a considerable contribution to  $\text{N}_2\text{O}$  production on a global scale [Dore *et al.*, 1998]. Therefore,  $\text{N}_2\text{O}$  yield during nitrification is a critical parameter in estimating  $\text{N}_2\text{O}$  production from models based on nitrification and/or remineralization rates. A simple reciprocal fit to the field measurements results in a systematically

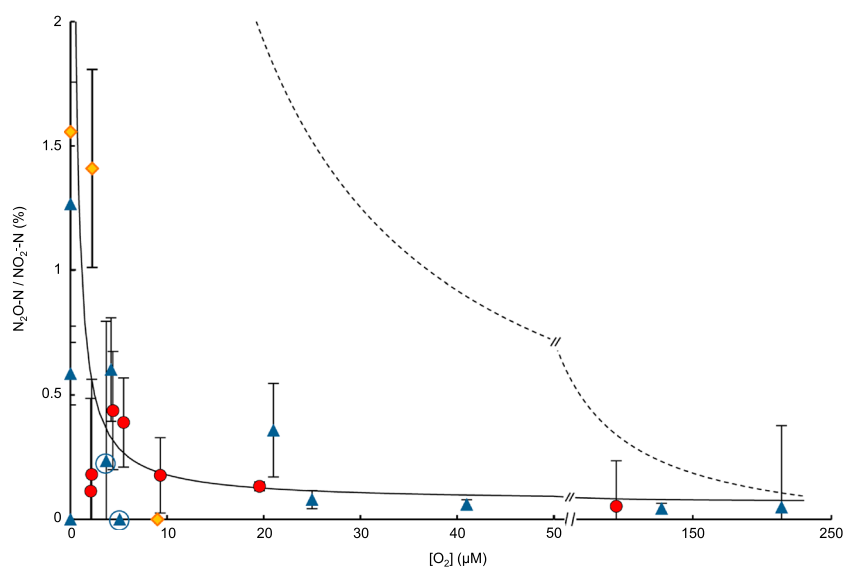


**Figure 2.**  $\text{N}_2\text{O}$  yield (in %), the ratio of  $\text{N}_2\text{O}$  production to  $\text{NO}_2^-$  production from  $\text{NH}_4^+$  oxidation, measured at depths where  $[\text{O}_2]$  varied from saturation to  $<10$  nM. Data are from upper oxycline at transect stations (circles), process stations (triangles), and  $[\text{O}_2]$  manipulation experiments (diamonds). Samples from process stations lower oxycline below the ODZ are shown as a triangle in a circle. An empirical reciprocal best fit of data (solid line) was derived for  $[\text{O}_2] > 10$  nM:  $\text{N}_2\text{O}$  Yield (%) =  $1.07/[\text{O}_2] (\mu\text{M}) + 0.072$  and compared to the equation proposed by Nevison *et al.* [2003] (dashed line).

lower yield compared to the yield equation of Nevison *et al.* [2003], which was calibrated with data from the culture study by Goreau *et al.* [1980] (Figure 2). Therefore, global  $\text{N}_2\text{O}$  production models (e.g. Zamora and Oschlies [2014]; Martinez-Rey *et al.* [2015]) can be improved by incorporating field data from different oceanic basins rather than relying on culture work alone.

In addition, the  $\text{N}_2\text{O}$  yield from field measurements had a similar range to that of AOB in culture experiments and higher than that of AOA cultures (Table S1). Further research is required to investigate the relative importance of bacterial and archaeal contribution to the global marine  $\text{N}_2\text{O}$  production.

### 3.3. Oxygen Driven $\text{N}_2\text{O}$ Cycling in the OMZ

The cycling of  $\text{N}_2\text{O}$  can be quantified using the  $\text{N}_2\text{O}$  residence time, i.e., the ratio of  $\text{N}_2\text{O}$  concentration to measured  $\text{N}_2\text{O}$  production rates. The calculated residence time at the surface and oxycline depths was 5.5–7 years, which was consistent with 1–10 years of water residence times in the ETSP upwelling region when mixing and advection were considered [Johnston *et al.*, 2014]. The high production rates coincided with undersaturated  $[\text{N}_2\text{O}]$  (~60% saturation) and resulted in the shortest residence times ( $<20$  day) within the ODZ, suggesting  $\text{N}_2\text{O}$  reduction and production must be cooccurring [Babbitt *et al.*, 2015].  $\text{N}_2\text{O}$  reduction is mediated by nitrous oxide reductase ( $\text{N}_2\text{OR}$ ), the most oxygen-sensitive enzyme in the denitrification pathway.  $\text{N}_2\text{OR}$  has the lowest oxygen inhibition concentration, likely at a few  $\mu\text{M}$  [Bonin *et al.*, 1989], whereas the enzymes nitrate reductase and nitrite reductase isolated from denitrifying bacteria had half-inhibition  $[\text{O}_2]$  of 21–25  $\mu\text{M}$ . [Körner and Zumft, 1989]. Thus,  $\text{N}_2\text{O}$  reduction is favored within the ODZ but the activity decreases in the presence of oxygen. At the oxic-anoxic interface, this critical low, but nonzero, oxygen concentration enhances  $\text{N}_2\text{O}$  production from both nitrification and denitrification, but inhibits  $\text{N}_2\text{O}$  consumption, resulting in the characteristic  $\text{N}_2\text{O}$  peak.

Slowest  $\text{N}_2\text{O}$  production at the lower oxycline where  $[\text{N}_2\text{O}]$  was high, indicated the longest residence time ( $>17$  years) in the water column.  $\text{N}_2\text{O}$  respiration may not be favorable likely due to low organic matter input and the presence of oxygen. Sluggish ventilation may be an important factor facilitating  $\text{N}_2\text{O}$  accumulation below the ODZ.

Due to decreased oxygen solubility by ocean warming, the marine oxygen minimum zones may potentially expand in the future [Stramma *et al.*, 2008]. Enhanced near-shore nitrogen loss rates are also possible due to increased input of anthropogenic organic matter. The resulting marine  $\text{N}_2\text{O}$  efflux is likely to increase,

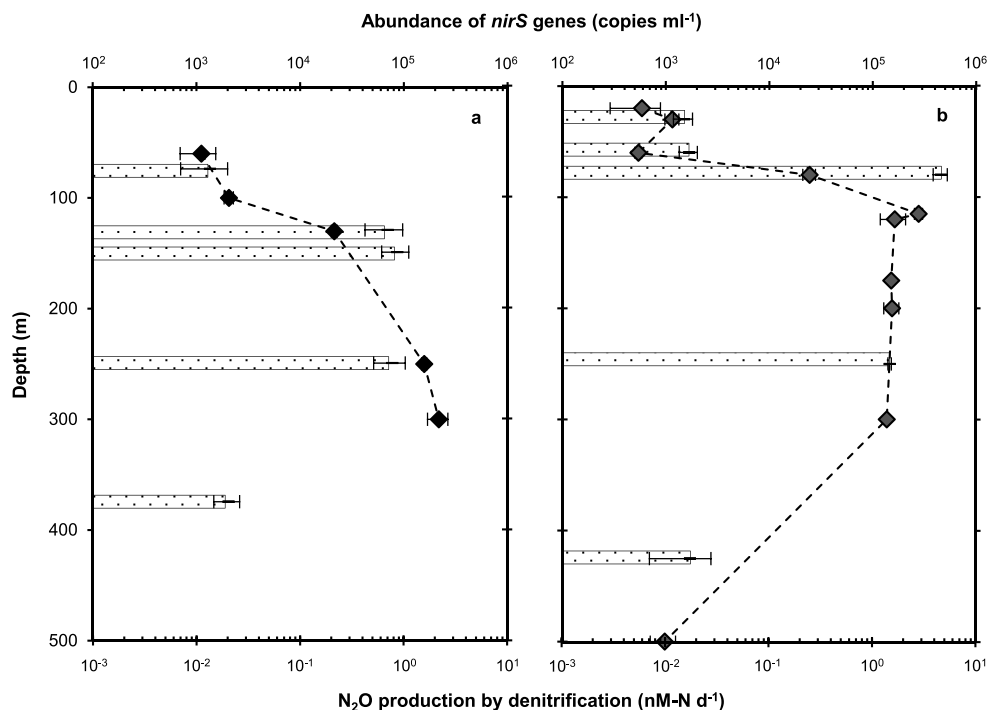


**Figure 3.** Distribution of *nirS* gene abundances (filled diamond with dashed line) and rates of  $N_2O$  production from denitrification (horizontal bars), defined as summation of  $NO_2^-$  and  $NO_3^-$  reduction to  $N_2O$ . Data from (a) offshore process station BB1 and (b) coastal process station BB2. Error bars on *nirS* abundances represent the standard deviation of the three replicates. The replicate values in most of the depths were so close to each other that error bars are not visible.

because (1) increase of areal coverage of low-oxygen waters enables elevated  $N_2O$  production from increasing  $N_2O$  yield from nitrification, (2) increasing temperature may enhance microbial enzymatic nitrification and denitrification at the oxic-anoxic interface and lead to enhanced  $N_2O$  production from both processes, and (3) shoaling of the upper oxycline and top of the ODZ where  $N_2O$  accumulates will increase surface  $N_2O$  supersaturation and thus increase efflux [Codispoti, 2010].

### 3.4. The *nirS* Gene as a Biomarker for Denitrifying Activity

The *nirS* gene abundance at both stations showed a gradual increase with depth and peaked within the ODZ (Figure 3). The abundance of *nirS* genes can be used as a proxy for the size of denitrifying community, assuming the *nirS* genes are present as a single copy per cell [Zumft, 1997]. The present analysis shows apparent covariation between the distributions of *nirS* genes and the measured  $N_2O$  production rates from denitrification ( $NO_2^-$  reduction plus  $NO_3^-$  reduction to  $N_2O$ ), suggesting that the size of denitrifying community is an indicator of denitrifying activity. Low *nirS* abundances ( $< 10^3$  copies  $mL^{-1}$ ) were observed at the surface and the oxycline below the ODZ, indicating that *nirS*-type denitrifying bacteria were rare outside the ODZ. However, detectable  $NO_2^-$  reduction to  $N_2O$  was observed in these regions, and at this point it is not clear which genes are involved in the  $N_2O$  production processes at oxygenated depths.

## 4. Conclusions

The Eastern Tropical South Pacific oxygen minimum zone is a region of intense  $N_2O$  production, as indicated by surface and subsurface  $N_2O$  supersaturation, and detection of active production from nitrification and denitrification. Rates of  $N_2O$  production from denitrification are much higher than from nitrification. Denitrification is important to the production in the OMZs and by extension, global fluxes. This suggests that  $N_2O$  flux models, which identify OMZs as the major sites of pelagic  $N_2O$  emissions, could represent the biogeochemistry more accurately by incorporating both nitrification and denitrification.

Oxygen is likely an important factor regulating nitrification and denitrification in  $N_2O$  production and consumption. For nitrification-derived  $N_2O$  production, the oxycline below the euphotic zone is the

important depth range, where the  $\text{N}_2\text{O}$  yield during nitrification increases with decreasing  $[\text{O}_2]$ , with highest yield ( $>1\%$ ) at  $[\text{O}_2] < 2 \mu\text{M}$ . Denitrification-derived  $\text{N}_2\text{O}$  production ( $\text{NO}_2^-$  and  $\text{NO}_3^-$  reduction to  $\text{N}_2\text{O}$ ) was active under suboxic conditions, where  $[\text{O}_2] < 10 \mu\text{M}$ . Therefore, at the oxic-anoxic interface, the highest  $\text{N}_2\text{O}$  production rates from both nitrification and denitrification contribute to peak  $\text{N}_2\text{O}$  concentrations in the water column. Anoxic conditions within the ODZ proper allowed a relatively large population of denitrifying bacteria to thrive, as indicated by high abundances of *nirS* genes and high rates of  $\text{N}_2\text{O}$  production from denitrification. Due to the release from oxygen inhibition, the consumption of  $\text{N}_2\text{O}$  by denitrification is more pronounced within the ODZ, such that in situ  $\text{N}_2\text{O}$  concentration is maintained at undersaturated levels. Therefore, anoxic conditions coinciding with  $\text{N}_2\text{O}$  undersaturation signal intense  $\text{N}_2\text{O}$  cycling with short turnover times leading to fixed nitrogen loss.

#### Acknowledgments

The authors would like to thank Calvin Mordy for providing seawater nutrient analysis, Niels Peter Revsbech for the STOX sensor data, Mark Warner for providing comparative shipboard  $\text{N}_2\text{O}$  concentration measurements, Osvaldo Ulloa and Gadiel Alarcón for the PPS operations, and Allan Devol for serving as chief scientist on R/V *Nathaniel M. Palmer*. In the preparation of the manuscript, Nicolas Van Oostende, Xuefeng Peng, and Jessica Lueders-Dumont provided valuable comments and suggestions. This research was supported by US-NSF grants to B.B.W. A.R.B. was additionally funded by a US-NSF Postdoctoral Research Fellowship in Biology (1402109). Supporting information can be found on website. The authors declare no conflict of interests.

#### References

- Anderson, J. H. (1964), The metabolism of hydroxylamine to nitrite by *Nitrosomonas*, *Biochem. J.*, *91*(1), 8–17.
- Arevalo-Martinez, D. L., A. Kock, C. R. Loscher, R. A. Schmitz, and H. W. Bange (2015), Massive nitrous oxide emissions from the tropical South Pacific Ocean, *Nat. Geosci.*, *8*(7), 530–533, doi:10.1038/ngeo2469.
- Babbin, A. R., R. G. Keil, A. H. Devol, and B. B. Ward (2014), Organic matter stoichiometry, flux, and oxygen control nitrogen loss in the ocean, *Science*, *344*(6182), 406–408, doi:10.1126/science.1248364.
- Babbin, A. R., D. Bianchi, A. Jayakumar, and B. B. Ward (2015), Rapid nitrous oxide cycling in the suboxic ocean, *Science*, *348*(6239), 1127–1129, doi:10.1126/science.aaa8380.
- Bianchi, D., J. P. Dunne, J. L. Sarmiento, and E. D. Galbraith (2012), Data-based estimates of suboxia, denitrification, and  $\text{N}_2\text{O}$  production in the ocean and their sensitivities to dissolved  $\text{O}_2$ , *Global Biogeochem. Cycles*, *26*, GB2009, doi:10.1029/2011GB004209.
- Bonin, P., M. Gilewicz, and J. C. Bertrand (1989), Effects of oxygen on each step of denitrification on *Pseudomonas nautica*, *Can. J. Microbiol.*, *35*(11), 1061–1064, doi:10.1139/m89-177.
- Canfield, D. E., F. J. Stewart, B. Thamdrup, L. De Brabandere, T. Dalsgaard, E. F. Delong, N. P. Revsbech, and O. Ulloa (2010), A cryptic sulfur cycle in oxygen-minimum-zone waters off the Chilean Coast, *Science*, *330*(6009), 1375–1378, doi:10.1126/science.1196889.
- Ciais, P., et al. (2013), *Carbon and Other Biogeochemical Cycles*, pp. 465–570, Cambridge Univ. Press, Cambridge, U. K., and New York.
- Codispoti, L. A. (2010), Interesting times for marine  $\text{N}_2\text{O}$ , *Science*, *327*(5971), 1339–1340, doi:10.1126/science.1184945.
- Codispoti, L. A., and J. P. Christensen (1985), Nitrification, denitrification and nitrous oxide cycling in the eastern tropical South Pacific ocean, *Mar. Chem.*, *16*(4), 277–300, doi:10.1016/0304-4203(85)90051-9.
- Cohen, Y., and L. I. Gordon (1978), Nitrous oxide in the oxygen minimum of the eastern tropical North Pacific: Evidence for its consumption during denitrification and possible mechanisms for its production, *Deep Sea Res., Part II*, *25*(6), 509–524, doi:10.1016/0146-6291(78)90640-9.
- Dalsgaard, T., B. Thamdrup, L. Fariás, and N. Peter Revsbech (2012), Anammox and denitrification in the oxygen minimum zone of the eastern South Pacific, *Limnol. Oceanogr.*, *57*(5), 1331–1346, doi:10.4319/lo.2012.57.5.1331.
- De Brabandere, L., B. Thamdrup, N. P. Revsbech, and R. Foadi (2012), A critical assessment of the occurrence and extend of oxygen contamination during anaerobic incubations utilizing commercially available vials, *J. Microbiol. Meth.*, *88*(1), 147–154, doi:10.1016/j.mimet.2011.11.001.
- Dore, J. E., B. N. Popp, D. M. Karl, and F. J. Sansone (1998), A large source of atmospheric nitrous oxide from subtropical North Pacific surface waters, *Nature*, *396*(6706), 63–66, doi:10.1038/23921.
- Frame, C. H., and K. L. Casciotti (2010), Biogeochemical controls and isotopic signatures of nitrous oxide production by a marine ammonia-oxidizing bacterium, *Biogeochemistry*, *7*(9), 2695–2709, doi:10.5194/bg-7-2695-2010.
- Freitag, A., D. W. Wallace, and H. W. Bange (2012), Global oceanic production of nitrous oxide, *Philos. Trans. R. Soc. London B Biol. Sci.*, *367*(1593), 1245–1255, doi:10.1098/rstb.2011.0360.
- Goreau, T. J., W. A. Kaplan, S. C. Wofsy, M. B. McElroy, F. W. Valois, and S. W. Watson (1980), Production of  $\text{NO}_2^-$  and  $\text{N}_2\text{O}$  by nitrifying bacteria at reduced concentrations of oxygen, *Appl. Environ. Microbiol.*, *40*(3), 526–532.
- Jayakumar, A., G. D. O'Mullan, S. W. Naqvi, and B. B. Ward (2009), Denitrifying bacterial community composition changes associated with stages of denitrification in oxygen minimum zones, *Microbial Ecol.*, *58*(2), 350–362, doi:10.1007/s00248-009-9487-y.
- Jayakumar, A., X. Peng, and B. Ward (2013), Community composition of bacteria involved in fixed nitrogen loss in the water column of two major oxygen minimum zones in the ocean, *Aquat. Microb. Ecol.*, *70*(3), 245–259, doi:10.3354/ame01654.
- Johnston, D. T., B. C. Gill, A. Masterson, E. Beirne, K. L. Casciotti, A. N. Knapp, and W. Berelson (2014), Placing an upper limit on cryptic marine sulphur cycling, *Nature*, *513*(7519), 530–533, doi:10.1038/nature13698.
- Körner, H., and W. G. Zumft (1989), Expression of denitrification enzymes in response to the dissolved oxygen level and respiratory substrate in continuous culture of *Pseudomonas stutzeri*, *Appl. Environ. Microbiol.*, *55*(7), 1670–1676.
- Law, C. S., and N. J. P. Owens (1990), Significant flux of atmospheric nitrous oxide from the northwest Indian Ocean, *Nature*, *346*(6287), 826–828.
- Lipschultz, F., S. C. Wofsy, B. B. Ward, L. A. Codispoti, G. Friedrich, and J. W. Elkins (1990), Bacterial transformations of inorganic nitrogen in the oxygen-deficient waters of the Eastern Tropical South Pacific Ocean, *Deep Sea Res., Part I*, *37*(10), 1513–1541, doi:10.1016/0198-0149(90)90060-9.
- Löscher, C. R., A. Kock, M. Könneke, J. LaRoche, H. W. Bange, and R. A. Schmitz (2012), Production of oceanic nitrous oxide by ammonia-oxidizing archaea, *Biogeochemistry*, *9*(7), 2419–2429, doi:10.5194/bg-9-2419-2012.
- Mantoura, R. F. C., and E. M. S. Woodward (1983), Optimization of the indophenol blue method for the automated determination of ammonia in estuarine waters, *Estuarine Coastal Shelf Sci.*, *17*(2), 219–224, doi:10.1016/0272-7714(83)90067-7.
- Martens-Habbena, W., P. M. Berube, H. Urakawa, J. R. de la Torre, and D. A. Stahl (2009), Ammonia oxidation kinetics determine niche separation of nitrifying archaea and bacteria, *Nature*, *461*(7266), 976–979, doi:10.1038/nature08465.
- Martinez-Rey, J., L. Bopp, M. Gehlen, A. Tagliabue, and N. Gruber (2015), Projections of oceanic  $\text{N}_2\text{O}$  emissions in the 21st century using the IPSL Earth system model, *Biogeochemistry*, *12*(13), 4133–4148, doi:10.5194/bg-12-4133-2015.
- McIlvin, M. R., and M. A. Altabet (2005), Chemical conversion of nitrate and nitrite to nitrous oxide for nitrogen and oxygen isotopic analysis in freshwater and seawater, *Anal. Chem.*, *77*(17), 5589–5595.
- Moir, J. W. B., and N. J. Wood (2001), Nitrate and nitrite transport in bacteria, *Cell. Mol. Life Sci.*, *58*(2), 215–224, doi:10.1007/PL00000849.

- Molina, V., and L. Fariás (2009), Aerobic ammonium oxidation in the oxycline and oxygen minimum zone of the eastern tropical South Pacific off northern Chile (~20°S), *Deep Sea Res., Part II*, 56(16), 1032–1041, doi:10.1016/j.dsr2.2008.09.006.
- Naqvi, S. W. A., and R. J. Noronha (1991), Nitrous oxide in the Arabian Sea, *Deep Sea Res., Part I*, 38(7), 871–890, doi:10.1016/0198-0149(91)90023-9.
- Naqvi, S. W. A., D. A. Jayakumar, P. V. Narvekar, H. Naik, V. V. S. S. Sarma, W. D'Souza, S. Joseph, and M. D. George (2000), Increased marine production of N<sub>2</sub>O due to intensifying anoxia on the Indian continental shelf, *Nature*, 408(6810), 346–349, doi:10.1038/35042551.
- Nevison, C., J. H. Butler, and J. W. Elkins (2003), Global distribution of N<sub>2</sub>O and the ΔN<sub>2</sub>O-AOU yield in the subsurface ocean, *Global Biogeochem. Cycles*, 17(4), 1119, doi:10.1029/2003GB002068.
- Nicholls, J. C., C. A. Davies, and M. Trimmer (2007), High-resolution profiles and nitrogen isotope tracing reveal a dominant source of nitrous oxide and multiple pathways of nitrogen gas formation in the central Arabian Sea, *Limnol. Oceanogr.*, 52(1), 156–168, doi:10.2307/40006070.
- Poth, M., and D. D. Focht (1985), (15)N kinetic analysis of N(2)O production by *Nitrosomonas europaea*: An examination of nitrifier denitrification, *Appl. Environ. Microbiol.*, 49(5), 1134–1141.
- Revsbech, N. P., L. H. Larsen, J. Gundersen, T. Dalsgaard, O. Ulloa, and B. Thamdrup (2009), Determination of ultra-low oxygen concentrations in oxygen minimum zones by the STOX sensor, *Limnol. Oceanogr. Methods*, 7, 371–381.
- Smith, C. J., D. B. Nedwell, L. F. Dong, and A. M. Osborn (2006), Evaluation of quantitative polymerase chain reaction-based approaches for determining gene copy and gene transcript numbers in environmental samples, *Environ. Microbiol.*, 8(5), 804–815.
- Stieglmeier, M., M. Mooshammer, B. Kitzler, W. Wanek, S. Zechmeister-Boltenstern, A. Richter, and C. Schleper (2014), Aerobic nitrous oxide production through N-nitrosating hybrid formation in ammonia-oxidizing archaea, *ISME J.*, 8(5), 1135–1146, doi:10.1038/ismej.2013.220.
- Stramma, L., G. C. Johnson, J. Sprintall, and V. Mohrholz (2008), Expanding oxygen-minimum zones in the tropical oceans, *Science*, 320(5876), 655–658, doi:10.1126/science.1153847.
- Suntharalingam, P., and J. L. Sarmiento (2000), Factors governing the oceanic nitrous oxide distribution: Simulations with an ocean general circulation model, *Global Biogeochem. Cycles*, 14(1), 429–454, doi:10.1029/1999GB900032.
- Thamdrup, B., T. Dalsgaard, and N. P. Revsbech (2012), Widespread functional anoxia in the oxygen minimum zone of the Eastern South Pacific, *Deep Sea Res., Part I*, 65, 36–45, doi:10.1016/j.dsr.2012.03.001.
- United Nations Educational, Scientific and Cultural Organization (1994), *Protocols for the Joint Global Ocean Flux Study (JGOFS) Core Measurements*, edited by I. O. Commission, United Nations Educational, Scientific and Cultural Organization.
- Ward, B. B. (2005), Temporal variability in nitrification rates and related biogeochemical factors in Monterey Bay, California, USA, *Mar. Ecol. Prog. Ser.*, 292, 97–109, doi:10.3354/meps292097.
- Ward, B. B., and O. C. Zafriou (1988), Nitrification and nitric oxide in the oxygen minimum of the eastern tropical North Pacific, *Deep Sea Res., Part A*, 35(7), 1127–1142, doi:10.1016/0198-0149(88)90005-2.
- Ward, B. B., C. B. Tuit, A. Jayakumar, J. J. Rich, J. Moffett, and S. W. A. Naqvi (2008), Organic carbon, and not copper, controls denitrification in oxygen minimum zones of the ocean, *Deep Sea Res., Part I*, 55(12), 1672–1683, doi:10.1016/j.dsr.2008.07.005.
- Wilson, S. T., D. A. del Valle, M. Segura-Noguera, and D. M. Karl (2014), A role for nitrite in the production of nitrous oxide in the lower euphotic zone of the oligotrophic North Pacific Ocean, *Deep Sea Res., Part I*, 85, 47–55, doi:10.1016/j.dsr.2013.11.008.
- Yoshida, N., H. Morimoto, M. Hirano, I. Koike, S. Matsuo, E. Wada, T. Saino, and A. Hattori (1989), Nitrification rates and <sup>15</sup>N abundances of N<sub>2</sub>O and NO<sub>3</sub><sup>-</sup> in the western North Pacific, *Nature*, 342(6252), 895–897, doi:10.1038/342895a0.
- Zamora, L. M., and A. Oschlies (2014), Surface nitrification: A major uncertainty in marine N<sub>2</sub>O emissions, *Geophys. Res. Lett.*, 41, 4247–4253, doi:10.1002/2014GL060556.
- Zumft, W. G. (1997), Cell biology and molecular basis of denitrification, *Microbiol. Mol. Biol. Rev.*, 61(4), 533–616.